Original Article

Numerical simulation and compact modeling of low voltage pentacene based OTFTs

A.D.D. Dwivedi[*], S.K. Jain, Rajeev Dhar Dwivedi, Shubham Dadhich

Department of Electrical and Electronics Engineering, Poornima University Jaipur, India

A B S T R A C T

As organic thin film transistors (OTFTs) are poised to play a key role in flexible and low-cost electronic applications, there is a need of device modeling to support technology optimization and circuit design. This paper demonstrates the technology computer-aided design (TCAD) based numerical simulation, compact modeling and parameter extraction of a low voltage Pentacene based OTFTs. In this paper, fundamental semiconductor equations are tuned up to represent the device electrical characteristics using device numerical simulation. We also present the compact device modeling and parameter extraction of low voltage pentacene based OTFT using the universal organic thin-film transistor (UOTFT) model. Results of finite element method based ATLAS simulation and compact modeling are validated with the experimental results of fabricated Pentacene based OTFT devices. Further, P-type TFT based inverter is also simulated to evaluate the compact model against a simple circuit simulation.

© 2019 The Authors. Publishing services by Elsevier B.V. on behalf of Vietnam National University, Hanoi. This is an open access article under the CC BY license (http://creativecommons.org/licenses/by/4.0/).

1. Introduction

The research in the area of organic thin-film/field effect transistors (OTFTs/OFETs) has been cultivating rapidly in recent years. Due to its low cost, light weight and very low manufacturing temperature, OTFTs have an ample range of applications, such as displays, sensors and radio frequency identification tags (RFIDs) [1,2]. Performance of an OTFT depends to a large extent on the gate insulator, the insulator/organic interface quality, the morphology of the organic film, and the process of charge injection. A significant progress has been made in terms of synthesizing a new organic semiconductor with improved electron/hole transport and injection properties as well as ambient stability [3]. Low-voltage Pentacene OTFTs with different gate dielectric interfaces have good electrical performance and operational stability [4]. Also, OTFTs fabricated with the crystals of TIPS-Pentacene show high electrical stability upon bending [5] and solution processed flexible OFETs with TIPS-Pentacene and polystyrene blend exhibit high electro-mechanical stability [6]. The OFET operates in the accumulation mode, where most of the modulation charges of the conduction path is located in the first monolayer next to the semiconductor -insulator interface. So the properties of the interface between the semiconductor and the gate dielectric have a great importance. Actually, stack of organic semiconductors (OSC), low temperature polymer gate dielectrics and the rapid annealing process are suitable with high-throughput for low cost printing manufacturing [7]. Device modeling for circuit simulation is usually done using a compact model that simulates the physical phenomena within the device using physical basis or empirical functions [8]. Polymers and small molecules indicate that the OSC has a great potential for improved performance through chemical structures and process optimization [9]. Recently, we have seen that Pentacene OTFT have made significant improvements in device performance and the performance of OTFTs can now be comparable to amorphous hydrogenated silicon (a:Si:H) TFTs [10]. However, this performance is not sufficient in comparison to inorganic TFTs. Lot of works is yet to be done to improve the electrical characteristic, uniformity and reliability. The process optimization of the device geometries and techniques requires basic numerical multidimensional models to control the charge distribution and the carrier transport in organic semiconductors. On the other hand, there is a need for an efficient and accurate compact model to work as a bridge between the OTFT technology and circuit designing.

In this paper, we use Silvaco's Atlas 2D simulator to explore the charge carrier continuity equation, the poisson's semiconductor device equation [11–20] and the drift diffusion model to simulate electrical characteristics of the given device. Silvaco's UTMOST-IV

model parameter extraction software is used to obtain compact model parameters using the UOTFT model. TCAD simulation and compact simulation results were also compared with those of an experimentally fabricated device. Compact models have been applied to logic circuit simulations and P-type TFT-based inverter circuits have been simulated using compact model parameters extracted from the UOTFT model. This article contains five parts. This section talks about basic introduction. Device structure and simulation are introduced in section II. Compact modeling, model validation, and parameter extraction are explained in the section III. Finally, conclusions drawn are given in section IV.

2. Numerical simulation

2.1. Device structure and simulation

The schematic of Pentacene based low voltage OTFT is given in Fig. 1. In the Schematic, a 5.3 nm thick gate dielectric consisting of a 3.6 nm thin aluminum oxide layer and a 1.7 nm thick n-tetrade-cylphosphonic acid self-assembled monolayer (SAM) provides a very high capacitance density of 600 nF/cm^2 [21]. Next, an organic semiconductor with thickness of 25 nm was deposited on the gate dielectric. Metal contacts were deposited on the top to define the source/drain electrodes. The width (W) and length (L) for this representation of device were 100 μm and 30 μm, respectively.

Pentacene is a routinely used organic semiconductor and it has an HUMO-LUMO energy gap of 2.25eV [22], which is suitable for the transistor operation with an Au electrode. For device simulation using ATLAS, the device structure with same dimension was replicated.

2.2. Device physical equation

The device structure of a Pentacene based OTFT as shown in Fig. 1 was created using ATLAS and its electrical characteristics were simulated. This simulator solves the continuity Poisson's equations and the charge transport equations [23,24] to obtain the desired characteristics of the OTFT. Various standard models like energy balance model and drift-diffusion (DD) model are used by ATLAS for the transportation of charge carriers. Fermi-Dirac Statistics and field-dependent mobility model were used for the carrier distribution and mobility. The Poisson equation determines the electric field intensity in the given device based on the internal movement of the carriers and the distribution of the fixed charges given by equation (1) [12−19].

$$\nabla.E = \frac{\rho}{\varepsilon} \tag{1}$$

where ρ is the charge density and ε is the permittivity of the region, ρ is given by
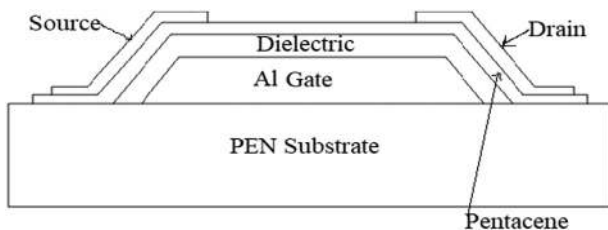

Fig. 1. Schematic cross−sectional diagram of OTFTs device.

$$\rho = q[p - n + N_D^+ - N_A^-] \tag{2}$$

where p is the hole density, n is the electron density, N_D^+ is the ionization donor density, and N_A^- is the ionization acceptor density. The continuity equations describing the dynamics of the charge carrier distribution over time are shown in equations (3) and (4) [12−19].

$$\frac{\partial n}{\partial t} = \frac{1}{q}\nabla.J_n + G_n - R_n \tag{3}$$

$$\frac{\partial p}{\partial t} = -\frac{1}{q}\nabla.J_p + G_p - R_p \tag{4}$$

where the symbols have their usual meanings. A third important set of equations for describing the device physics for the charge carriers are the drift-diffusion equations given as

$$J_p = qn\mu_p E - qD_p\nabla p \tag{5}$$

$$J_n = qn\mu_n E + qD_n\nabla n \tag{6}$$

2.3. Density of states and the model of the trapped carrier density

In the disordered organic semiconductor material various defect states are present in the band gap that trap the charge carriers. So we have included the energy distribution of the defect states also. To account for the trapped charge, Poisson's equations are modified by adding an additional term Q_T, representing the trapped charges given in equation (7) [12−19,25].

$$\rho = q(p - n + N_D^+ - N_A^-) + Q_T \tag{7}$$

where $Q_T = q(p_T - n_T)$. Here, p_T and n_T are the ionized density of donor like traps and the ionized density of acceptor like traps, respectively and p_T = total density states $\times f_{tD}$ and n_T = total density states $\times f_{tA}$ where f_{tD} and f_{tA} are the probabilities of ionization of the donor like and accepter like traps, respectively. The total density of defect states (DOS) $g(E)$, also governs the properties of OTFTs which is modeled as consisting of four constituents *i.e.* a donor-like exponential band tail function $g_{TD}(E)$, an acceptor like exponential band tail function $g_{TA}(E)$, a donor like Gaussian deep state function $g_{GD}(E)$, an acceptor like Gaussian deep state function $g_{GA}(E)$ and where E is the trap energy. The equations describing these terms are given as follows [12−19]:

$$g_{TA}(E) = N_{TA}\exp\left[\frac{E - E_c}{W_{TA}}\right] \tag{8}$$

$$g_{TD}(E) = N_{TD}\exp\left[\frac{E_v - E}{W_{TD}}\right] \tag{9}$$

$$g_{GA}(E) = N_{GA}\exp\left[-\left[\frac{E_{GA} - E}{W_{GA}}\right]^2\right] \tag{10}$$

$$g_{GD}(E) = N_{GD}\exp\left[-\left[\frac{E - E_{GD}}{W_{GD}}\right]^2\right] \tag{11}$$

E is the trap energy, E_C is the conduction band energy and E_V is the valence band energy and the subscripts T,G,A,D represent

the tail, Gaussian (depth), acceptor and donor states, respectively. For the exponential tails, DOS is described by its conduction and valence band edge intercept densities (N_{TA} and N_{TD}) and its characteristic attenuation energy (W_{TA} and W_{TD}). For the Gaussian distribution, DOS is described by its total state density (N_{GA} and N_{GD}), its characteristic attenuation energy (W_{GA} and W_{GD}), and its peak energy distribution (E_{GA} and E_{GD}). As Pentacene based OTFT is the p-type OTFT so we consider only donor like states. So $g(E)$ is given as

$$g(E) = g_{TD}(E) + g_{GD}(E) \tag{12}$$

The trapped charge n_T is given by:

$$n_T = \int_{E_v}^{E_c} g(E).f(E,n,p)dE \tag{13}$$

where

$$f(E,n,p) = \frac{v_p\sigma_{T,p} + v_n\sigma_{T,n}.n_i\exp\left[\frac{E-E_i}{kT}\right]}{v_n\sigma_{T,n}\left(n + n_i\exp\left[\frac{E-E_i}{kT}\right]\right) + v_p\sigma_{T,p}\left(p + n_i\exp\left[\frac{E_i-E}{kT}\right]\right)} \tag{14}$$

$f(E,n,p)$ is defined as the ionization probability of the donors DOS, v_n is the thermal velocity of electrons, v_p is the thermal velocity of holes, and n_i is the intrinsic carrier concentration. $\sigma_{T,n}$ and $\sigma_{T,p}$ are the electron and hole capture cross sections, respectively.

2.4. Mobility model

In organic semiconductors charge transport occurs due to the hopping of the charge carriers in between the localized states. The mobility independent of field is given by equation (15) [26,27].

$$\mu_0 = \frac{qv_0}{kT}n_t^{-2/3}\exp\left[-2k\left(\frac{3X}{4\pi n_t}\right)^{1/3}\right] \tag{15}$$

where the attempt to the jump frequency is given by v_0, X symbolizes the percolation constant, k is the reciprocal of the career localization radius and n_t is the effective transport energy. At a high electric field, the mobility will be calculated using the Poole-Frenkel mobility model [28]. given below

$$\mu(E) = \mu_0\exp\left[-\frac{\Delta E_a}{kT} + \left(\frac{\beta}{kT} - \gamma\right)\sqrt{E}\right] \tag{16}$$

The field dependent mobility is given by $\mu(E)$ and the zero field mobility is given by μ_0, the zero field activation energy is given by ΔE_a, the Poole-Frankel factor is β, and the fitting parameter is γ. The electric field is denoted by E, k is the Boltzmann constant and T denotes the temperature. The thermionic emission and Poole Frankel barrier lowering were included in the ATLAs simulations also.

2.5. Material parameters used for Pentacene

The Pentacene based OTFT is designed in a bottom-gate, top-contact configuration. The designed structure has a channel length of 30 μm and a channel width of 100 μm as shown in Fig. 1. For the simulation of the Pentacene based OTFT structure [21], parameters used in simulation are listed in Table 1.

Table 1
Simulation Parameters of Pentacene based low voltage OTFT.

Material Simulation Parameters	Value
Thickness of pentacene	25 nm [21]
Dielectric thickness	5.3 nm [21]
Energy Band Gap (eV)	2.25 eV [22]
Electron affinity (eV)	2.49eV [29]
Intrinsic p-type doping	$2 \times 10^{17} cm^{-3}$ [30]
Work Function of aluminum Gate	4.1 eV [31]
Work Function of Au contact	5.0 eV [31]
N_{TA}	9×10^{12} cm^{-3} eV^{-1}
N_{TD}	4.5×10^{12} cm^{-3} eV^{-1}
W_{TA}	0.3eV
W_{TD}	0.5eV
W_{GA}	0.15eV
W_{GD}	0.15eV
E_{GA}	0.5eV
Electron mobility	7×10^{-4} cm^2/V−s
Hole mobility	0.54 cm^2/V−s
Pool Frankel Factor (betap.pfmob)	7.758×10^{-8} eV(V/cm)$^{1/2}$
ΔE_a is the zero field activation energy	1.792×10^{-7} eV

2.6. Comparison of TCAD simulated results with the experimental data

Fig. 2(a) shows the transfer characteristics obtained from the TCAD simulation of the Pentacene based OTFTs and their experimentally measured data. The transfer characteristics are obtained by varying the gate to source voltage (V_{GS}) from 0V to -3V keeping the drain voltage constant at -3V. There is a very good agreement between the simulated transfer characteristics and the experimental ones of the fabricated device. Fig. 2(b) shows the output characteristics obtained from the TCAD simulation of the Pentacene based OTFT and the experimentally measured output characteristics of it. The output characteristics were obtained by varying the drain to source voltage (V_{DS}) from 0V to −3V keeping the gate to source voltage (V_{GS}) constant at-1.5V, −1.8V, −2.1V, −2.4V, −2.7V and −3.0V. The simulated output characteristics matched with the experimentally measured data.

3. Compact modeling, parameter extraction and model verification

3.1. Compact modeling

Operation in the carrier accumulation mode, the exponential density of states, the interface traps and the space charge-limited carrier transport, the nonlinear parasitic resistance, the source and drain contacts without junction isolation, the dependence of the mobility on the carrier concentration, the electric field and temperature are the various unique features that require a dedicated compact TFT model. The Universal Organic TFT (UOTFT) model [20] is a modeling expression that extends the uniform charge control model (UCCM) [20,32] to OTFTs and introduces general expression of modeling for conductivity of channel of OTFTs [27,33,34]. In this way, the UOTFT model is applicable to various OTFT device architectures, specifications of material and manufacturing technologies. The equivalent circuit of the UOTFT Model is given in Fig. 3.

The control equation for the UOTFT model for the n-channel OTFT case is described here. The p-channel condition can be obtained by the direct change in the voltage, the charge polarity and the current.

The charge accumulation in channel per unit area at zero-channel potential ($-Q_{acc}$)$_0$ is calculated by the help of solution of the UCCM equation [23] given by following equations.
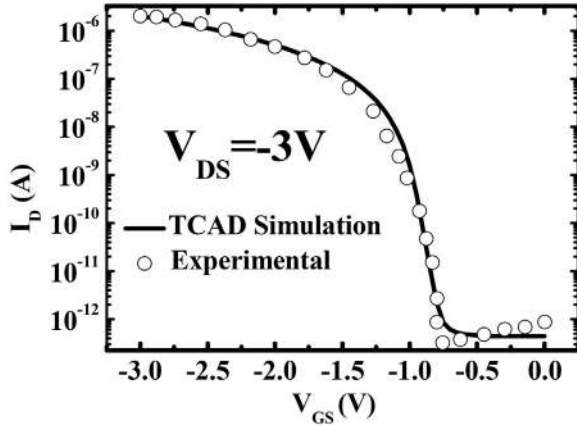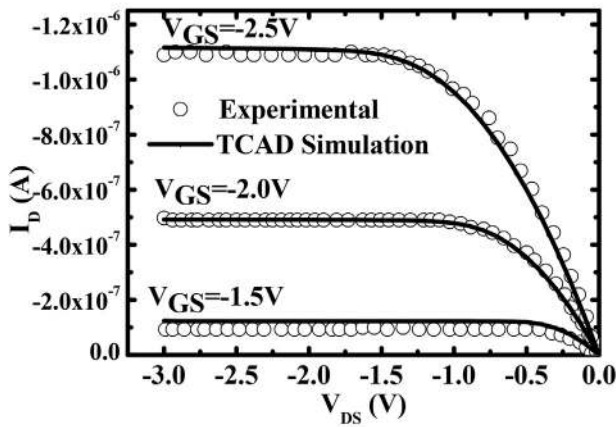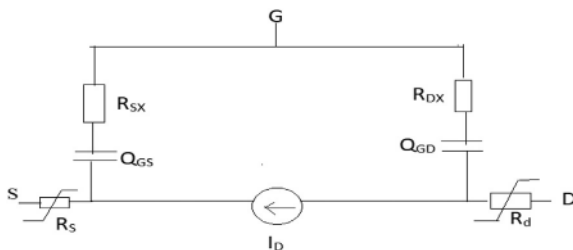
Fig. 2. (a) Comparisons of transfer characteristics of the TCAD simulated results and the measured data (b) Comparisons of Output characteristics obtained from TCAD simulation and the measured output characteristics.

$$(-Q_{acc})_o = C_i \cdot V_{gse} \tag{17}$$

$$V_{gse} = V_0(T) \cdot \ln\left[1 + \frac{e^{u+1}}{1 + k(u+2)\ln(1 + e^{u+1})}\right] \tag{18}$$

$$\text{where } u = \frac{V_{gs} - V_T(T)}{V_0(T)}$$

Fig. 3. Equivalent circuit of UOTFT Model.

$$C_i = \epsilon_0 \frac{\epsilon_r}{t_i} \tag{19}$$

where C_i is the gate insulator capacitance per unit area, V_{gse} is the effective intrinsic gate source voltage, V_{gs} is the gate-source voltage (intrinsic), V_T is the temperature-dependent threshold voltage parameter, and V_O is the characteristic voltage (temperature dependent) for the carrier density of states including the influence of the interface traps, ϵ_0 is the vacuum permittivity, and ϵ_r and t_i are model parameters representing the relative permittivity and thickness of the gate insulator, respectively.

3.1.1. Effective channel mobility

For an accurate modeling of OTFTs, the power-law characteristic dependence of the mobility on the carrier concentration is needed. According to the results of percolation theory [27], effective channel mobility is expressed in the UOTFT model as:

$$\mu_C = \mu_{eff} \cdot \left(\frac{(-Q_{acc})_0}{C_i \cdot V_{acc}}\right)^\alpha \tag{20}$$

μ_{eff}, V_{acc} and α are model parameters. μ_{eff} is a temperature-related parameter which defines the effective channel mobility at the onset of the channel strong accumulation. This onset point is controlled by the model parameter V_{acc} and is defined as the characteristic voltage of the effective mobility. The power-law dependence of the mobility on the carrier concentration is defined by the temperature-dependent model parameter α.

3.1.2. Intrinsic drain-source current

The drain-source current of the intrinsic transistor due to the charge carriers accumulated in the channel is defined by the following general interpolation expressions [20].

$$I_{ds}^{acc} = G_{ch} \cdot V_{dse} \tag{21}$$

$$V_{dse} = \frac{V_{ds}}{\left[1 + \left(\frac{G_{ch} \cdot V_{ds}}{I_{sat}(1 + \lambda V_{ds})}\right)^m\right]^{\frac{1}{m}}} \tag{22}$$

here G_{ch} is the effective channel conductance in the linear region, V_{dse} is the effective intrinsic drain source voltage, V_{ds} is the intrinsic drain source voltage, the parameter λ defines the finite output conductance in the saturation region, and m is the model parameter that provides a smooth transition between the linear and saturated transistor operation, i.e. called as Knee shape parameter. I_{sat} is the ideal intrinsic drain-source saturation current and the effective channel conductance in the linear region G_{ch} is obtained by the following way:

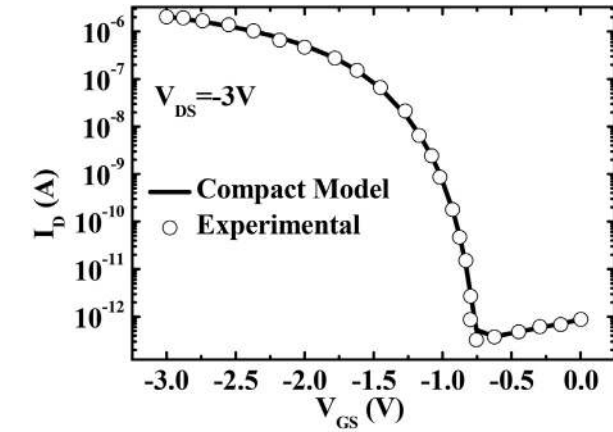$$G_{Ch} = \frac{G_{ch0}}{1 + G_{cho} \cdot R_{ds}} \tag{23}$$

$$G_{ch0} = \frac{W_{eff}}{L_{eff}} \cdot \mu_{c} \cdot (-Q_{acc})_0 \tag{24}$$

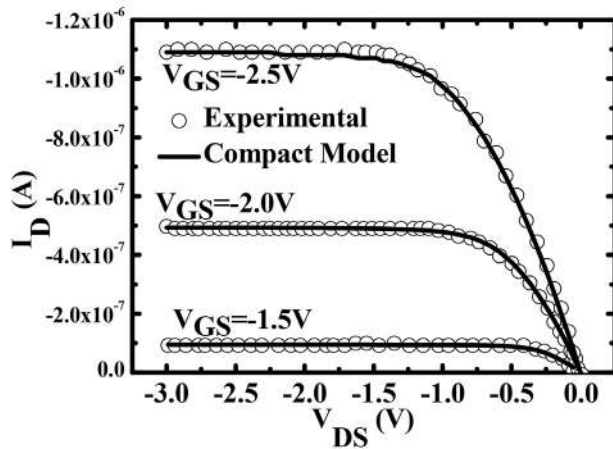The drain saturation current I_{sat} is determined by the following formula:

$$I_{sat} = G_{ch} \cdot V_{sat} \tag{25}$$

where V_{sat} is the saturation voltage.

The total intrinsic drain source–source current is given by following:

Fig. 4. (a) Comparisons of the transfer characteristics of the experimentally measured with the compact model based simulated data (b) Comparisons of the output characteristics of the experimentally measured with the compact model based simulated data.

$$I_{ds} = I_{ds}^{acc} + I_{ds}^{leak} \qquad (26)$$

where I_{ds} is total current and I_{ds}^{acc} is the accumulated current and I_{ds}^{leak} is the leakage current.

3.2. Comparison between the experimental and the compact model based simulated characteristics

Fig. 4(a) shows the comparison between the transfer characteristics obtained from experimentally measured data and the compact model based simulated characteristic of the Pentacene based OTFT [21]. The transfer characteristics are obtained by varying the gate to source voltage (V_{GS}) from 0V to −3V keeping the drain voltage constant at −3.0V.

Fig. 4(b) shows the output characteristics obtained from experimentally measured data and the compact model based simulated characteristic of the Pentacene based OTFT [21]. The output characteristics is obtained by varying the drain to source voltage (V_{DS}) from 0V to −3V keeping the gate to source voltage (V_{GS}) constant at-1.5V, −2.0V, −2.5V. There is a very good agreement between the experimentally measured and the compact model based simulated transfer and output characteristic of Pentacene based OTFT.

3.3. Parameter extraction

Extracted OTFT model parameters for the Pentacene based low voltage OTFT using the UOTFT model are given in Table 2. The extraction process starts with the collection of data for the I_D−V_{GS} and I_D−V_{DS} characteristics and providing it in UTMOST IV data base in. uds format. Further simulation of I_D−V_{DS} and I_D−V_{GS} characteristic using the UOTFT model and optimization of this characteristic using Levenberg Marquardt optimization technique with respect to the experimental data for extraction of model parameters have been performed. Extracted model parameters are listed in Table-II.

3.4. Simulation of logic circuit

For the UOTFT model validity, simple logic circuit was modeled based on p-type OTFTs only. The schematic in Fig. 5(a) shows the simple inverter circuit used in the simulation of a load transistor with auxiliary gate voltage (V_{aux}). The given inverter circuit works like a potential divider between the driver and the load OTFT. When the input voltage is lower than the threshold voltage (i.e. more positive than V_T), the driver OTFT turns off. On the other side, when it is more than the threshold voltage (i.e. more negative than V_T), the driver OTFT turns on. The operation of the inverter also depends on the load TFT size relatively with the driver TFT. To assess whether the simulation correctly reproduces this dependence, the size of load OTFT and its gate voltage (V) remain at the same value, while the size and gate voltage of driver OTFT changes. Fig. 5(b) shows the voltage transfer characteristics (V_{TC}) plot of the inverter

Table 2
Model Parameters extracted for UOTFT Model.

| Parameter Name	Symbol	UNIT	Values
The thickness of gate insulator	t_i	m	5.3×10^{-9}
Relative dielectric permittivity of the insulator at gate	ε_r	−	3.37
Relative dielectric permittivity of the semiconductor	ε_{sc}	−	4.0
Zero bias threshold voltage	V_T	V	−0.69
Trap density states Characteristic voltage	V_0	V	0.0082
Characteristic effective accumulation channel mobility	μ_{eff}	m^2/Vs	0.00061
Characteristic voltage of the effective mobility	V_{acc}	V	1.43
Output conductance parameter	λ	1/V	0.004
Knee shape parameter	m	−	1
Saturation modulation parameter	a	−	0.053
Leakage saturation current	I_{OL}	A	7.6e-19
Contact Resistance	$R_S + R_D$	Kilo Ohm	413.8
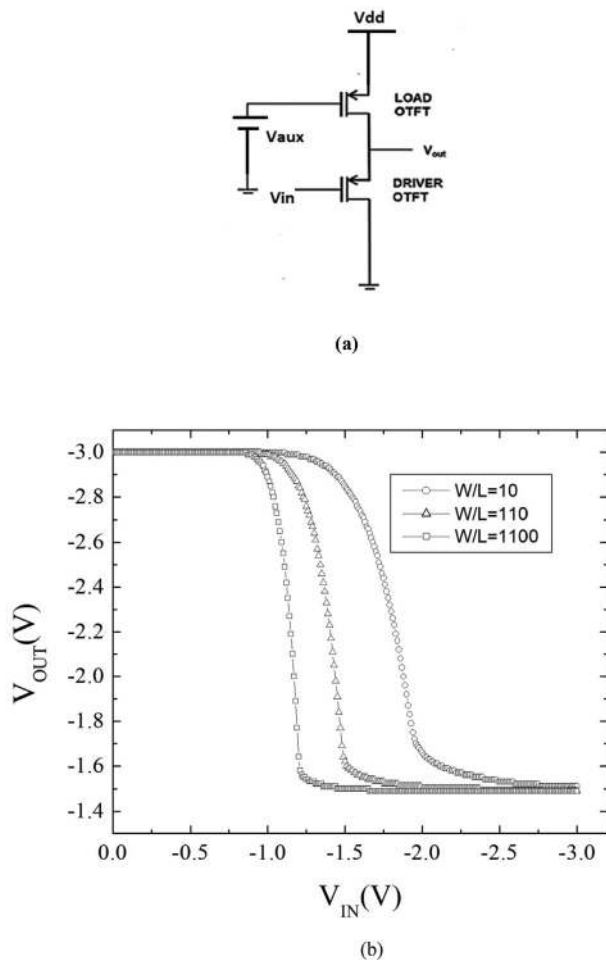
Fig. 5. (a) A circuit diagram of the inverter circuit used for assessing the simulation results (b) Voltage transfer characteristics of inverter circuit shown for different W/L ratios of driver OTFT.

circuit under consideration for W/L ratio of 10, 100 1100 of driver TFT. As W/L ratio of the driver OTFT increases, its impedance decreases and the transition between high and low states becomes clearer.

4. Conclusion

We presented a TCAD based numerical simulation, compact modeling using the UOTFT model and the model parameter extraction for Pentacene based OTFTs. TCAD simulation uses the field dependent mobility model and the density of defect states model with two exponential tail states and two Gaussian deep states. We simulated an OTFT based on Pentacene and demonstrated the application of the UOTFT model to organic TFTs and also used the experimental data from Pentacene-based OTFTs to extract parameters for the UOTFT compact model. It has been concluded that the UOTFT compact model provides more accurate modeling of OTFTs and the simpler parameter extraction methods for various organic OTFTs. The results show that the UOTFT model correctly simulates the behavior of the devices reported in this study and is expected to be used for more complex circuits based on organic thin film transistors. We also conclude that TCAD simulations, experimental results and compact model based simulation results of the electrical characteristic of Pentacene based TFT demonstrate the same behavior.

References

[1] P. Mach, S.J. Rodriguez, R. Nortrup, P. Wiltzius, J.A. Rogers, "Monolithically integrated, flexible display of polymer dispersed liquid crystal driven by rubber-stamped organic thin-film transistors", Appl. Phys. Lett. 78 (2001) 3592–3594.
[2] T. Someya, T. Sakurai, "Integration of organic field-effect transistors and rubbery pressure sensors for artificial skin applications", in: IEEE International Electron Devices Meeting, December, 2003, pp. 203–206.
[3] Y. Zhao, Y. Guo, Y. Liu, "25th anniversary article: recent advances in n-type and ambipolar organic field-effect transistors", Adv. Mater. 25 (2013) 5372–5391.
[4] Xiao-Hong Zhang, Shree Prakash Tiwari, Bernard Kippelen "Pentacene organic field-effect transistors with polymeric dielectric interfaces: performance and stability", Org. Electron. 10 (2009) 1133–1140.
[5] Vivek Raghuwanshi, Deepak Bharti, Shree Prakash Tiwari, "Flexible organic field-effect transistors with TIPS-Pentacene crystals exhibiting high electrical stability upon bending", Org. Electron. 31 (2016) 177–182.
[6] Deepak Bharti, Vivek Raghuwanshi, Ishan Varun, Ajay Kumar Mahato, Shree Prakash Tiwari, "High performance and electro-mechanical stability in small molecule: polymer blend flexible organic field-effect transistors", 37, 2016, pp. 1215–1218.
[7] Luisa Petti, Niko Münzenrieder, Christian Vogt, Hendrik Faber, Lars Büthe, Giuseppe Cantarella, Francesca Bottacchi, D. Thomas, Anthopoulos, and Gerhard Tröster, "Metal oxide semiconductor thin-film transistors for flexible electronics", Appl. Phys. Rev. 3 (2016), 021303.
[8] Ognian Marinov, M. Jamal Deen, , Fellow, IEEE, ute zschieschang, hagen klauk, "organic thin-film transistors:Part I—compact DC modeling", IEEE Trans. Electron Devices 56 (2009) 2952–2961.
[9] B.H. Lee, G.C. Bazan, A.J. Heeger, "Doping-induced carrier density modulation in polymer field-effect transistors", Adv. Mater. 28 (2016) 57–62.
[10] G. Horowitz, "Organic thin film transistors: from theory to real devices", J. Mater. Res. 19 (2004) 1946–1962.
[11] A. Buonomo, C. di, Bello "On solving Poisson's equation in two-dimensional semiconductor devices", Electron. Lett. 20 (1984) 156–158.
[12] Sumit Vyas, A.D.D. Dwivedi, Rajeev Dhar Dwivedi , "Effect of gate dielectric on the performance of ZnO based thin film transistor", Superlattice Microstruct. 120 (2018) 223–234.
[13] A.D.D. Dwivedi, Rajeev Dhar Dwivedi, Raghvendra Dhar Dwivedi, Sumit Vyas, P. Chakrabarti, Numerical simulation of P3HT based organic thin film transistors (OTFTs), Int. J. Microelectron. Digital Integrated Circ. 1 (2015) 13–20.
[14] A.D.D. Dwivedi, "Numerical simulation and spice modeling of organic thin film transistors" (OTFTs), Int. J. Adv. Appl. Phys. Res. 1 (2014) 14–21.
[15] Pooja Kumari, A.D.D. Dwivedi, "Modeling and simulation of pentacene based organic thin film transistors with organic gate dielectrics", Journal of Microelectronics and Solid State Devices 4 (2017) 13–18.
[16] Narendra Singh Kushwah, A.D.D. Dwivedi, "Computer modeling of organic thin film transistors (OTFTs) using verilog-A", Journal of Microelectronics and Solid State Devices 5 (2018) 1–7.
[17] A.D.D. Dwivedi, Pooja Kumari, "Numerical simulation and characterization of pentacene based organic thin film transistors with top and bottom gate configurations", Global Journal of Research in Engineering-F 19 (2019) 7–12.
[18] A.D.D. Dwivedi, Pooja Kumari, "TCAD simulation and performance analysis of single and dual gate OTFTs", Surf. Rev. Lett. (2019) 1950145, https://doi.org/10.1142/S0218625X19501452, 1-7.
[19] A.D.D. Dwivedi, Rajeev Dhar Dwivedi, Raghvendra Dhar Dwivedi, Qingda Zhao, "Technology computer aided design (TCAD) based simulation and compact modeling of Organic Thin Film Transistors (OTFTs) for circuit simulation", International Journal of Advanced Applied Physics Research 6 (2019) 1–5.
[20] A. Fjeldly, T. Ytterdal, M. Shur, "Introduction to Device Modeling and Circuit Simulation", Wiley, New York, NY, USA, 1998.
[21] Sibani Bisoyi, Shree Prakash Tiwari, Ute Zschieschang, and Hagen Klauk "Influence of gate and drain bias on the bias-stress stability of flexible organic thin-film transistors", in: Proceedings of 2nd IEEE International Conference on Emerging Electronics (ICEE 2014), Indian Institute of Science, Bangalore, India, 2014. December 03 - 06.

[22] L. Sebastian, G. Weiser, H. Bässler, "Charge transfer transitions in solid tetra-cene and pentacene studied by electroabsorption", Chem. Phys. 61 (1981) 125–135.

[23] W. van Roosbroeck, "Theory of the flow of electrons and holes in germanium and other semiconductors", Bell System Tech. J 29 (1950).

[24] A. Juengel, "Drift-diffusion Equations", Springer, 2009, pp. 99–127. Chap. 5.

[25] SILVACO, ATLAS User's Manual - Device Simulation Software USA, 2018.

[26] Han Chuan Yu, Ma Yuan Xiao, Tang Wing Man, Wang Xiao Li, P.T. Lai, "A study on pentacene organic thin-film transistor with different gate materials on various substrates", IEEE Electron. Device Lett. 38 (2017) 744–747.

[27] M.C.J.M. Vissenberg, "Theory of the field-effect mobility in amorphous organic transistors" M. Matters, Phys. Rev. B 57 (1998) 12964.

[28] C.H. Shim, F. Maruoka, R. Hattori, "Structural analysis on organic thin-film transistor with device simulation", IEEE Trans. Electron Devices 57 (2010) 195–200.

[29] E.A. Silinish, V. Čápek, Organic Molecular Crystals, Their Electronic States., New York, 1980.

[30] A.R. Brown, C.P. Jarrett, D.M. de Leeuw, M. Matters, "Field-effect transistors made from solution-processed organic semiconductors", Synth. Met. 88 (1997) 37–55.

[31] T. Zaki, S. Scheinert, I. Hörselmann, R. Rödel, F. Letzkus, H. Richter, U. Zschieschang, H. Klauk, J.N. Burghartz, "Accurate capacitance modeling and characterization of organic thin-film transistors", IEEE Trans. Electron Devices 61 (2014) 98–104.

[32] B. Iniguez, R. Picos, D. Veksler, A. Koudymov, M.S. Shur, T. Ytterdal, W. Jackson, "Universal compact model for long- and short-channel thin-film transistors", Solid State Electron. 52 (2008) 400–405.

[33] M. Estrada, A. Cerdeira, J. Puigdollers, L. Resendiz, J. Pallares, L.F. Marsal, C. Voz, B. Iñinguez, "Accurate modeling and parameter extraction for organic TFTs", Solid State Electron. 49 (2005) 1009–1016.

[34] UTMOST IV Spice Models Manual, Silvaco International, Santa Clara, CA,USA, 2018.